



Fermi National Accelerator Laboratory

**FERMILAB Conf-94/154-E
CDF**

Production Properties of Z Bosons with Jets in 1.8 TeV $p\bar{p}$ Collisions

The CDF Collaboration

*Fermi National Accelerator Laboratory
P.O. Box 500, Batavia, Illinois 60510*

May 1994

Submitted to the *27th International Conference on High Energy Physics*, Glasgow, Scotland, July 21-27, 1994

Disclaimer

This report was prepared as an account of work sponsored by an agency of the United States Government. Neither the United States Government nor any agency thereof, nor any of their employees, makes any warranty, express or implied, or assumes any legal liability or responsibility for the accuracy, completeness, or usefulness of any information, apparatus, product, or process disclosed, or represents that its use would not infringe privately owned rights. Reference herein to any specific commercial product, process, or service by trade name, trademark, manufacturer, or otherwise, does not necessarily constitute or imply its endorsement, recommendation, or favoring by the United States Government or any agency thereof. The views and opinions of authors expressed herein do not necessarily state or reflect those of the United States Government or any agency thereof.

Production Properties of Z Bosons with Jets in 1.8 TeV $\bar{p}p$ Collisions

The CDF Collaboration [1]

Abstract

We have measured the production of Z bosons from 1.8 TeV $\bar{p}p$ collisions using 19.3 pb^{-1} of integrated luminosity collected by the CDF during the 1992-93 Tevatron run. The production properties of the hadronic jets associated with the Z bosons are compared to leading-order QCD calculations using the VECBOS Monte Carlo program. For a subsample of events, B jets are identified using CDF's silicon tracker, and the rates compared to those expected from events with generic QCD jets.

Submitted to the 27th International Conference on High Energy Physics,
Glasgow, Scotland, July 21-27, 1994
Contribution Code: gls0419

1 Introduction

The production of Z bosons in high energy $\bar{p}p$ collisions provides a clean sample of events in which the primary parton scattering process is well defined. These data can be used to test QCD calculations of inclusive Z production properties (p_T and rapidity spectra) and the characteristics of the associated hadronic jets. The analysis presented here uses $Z + n$ jet events with $n = 1, 2$ and 3 to test leading order QCD predictions of the jet production properties. The data, collected by the CDF collaboration during the 1992-93 Tevatron run, uses Z bosons identified via the $Z \rightarrow e^+e^-$ and $Z \rightarrow \mu^+\mu^-$ decay modes. Details of the Z boson and jet selection are described in Section 2.

The measured jet production properties are compared to leading order QCD matrix element calculations. A Monte Carlo program, called VECBOS [2], is used to predict inclusive $Z + 1, 2$ and 3 parton events with the infrared and colinear divergences regularized by cuts on the minimum parton p_T and the separation between partons. These parton-level events are then passed through fragmentation algorithms which produce the complete particle structure of jets. After this the events are introduced into a model of the CDF detector which simulates the response of the electromagnetic and hadronic calorimeters and the muon detectors. The output of this simulation is in the same format as real data, and is passed through the same analysis cuts. Details of this Monte Carlo procedure are described in Section 3.

The analysis presented here compares the E_T spectra of the jets measured in our data to those predicted by the VECBOS-fragmentation-detector simulation. We find generally good agreement between the VECBOS predictions and our data. These results are presented in Section 4.

2 The Data Sample

The event sample used to select the $Z \rightarrow e^+e^-$ and $Z \rightarrow \mu^+\mu^-$ decays is extracted from 1.8 TeV $\bar{p}p$ collisions with an integrated luminosity of 19.3 pb^{-1} , collected by the CDF detector [3] in 1992-93. The momenta of charged particles are measured in a central tracking chamber (CTC) which is immersed in a 1.4 tesla magnetic field. Outside the CTC, electromagnetic and hadronic calorimeters, in a projective tower geometry, cover the pseudorapidity region $|\eta| < 3.6$. These calorimeters are used to identify jets and electron candidates. Outside the calorimeters, drift chambers in the region $|\eta| < 1.0$ provide muon identification. A silicon vertex detector (SVX) is located outside the beampipe and can be used to identify secondary vertices produced by b and c quark decays.

2.1 The $Z \rightarrow e^+e^-$ Data Set

The $Z \rightarrow e^+e^-$ decays are selected from a data set which includes all events with one high energy electron in the region $|\eta| < 1.0$. Level 3 of the on-line trigger requires that a reconstructed track with $p_T > 13$ GeV/c point to a reconstructed electromagnetic calorimeter cluster with $E_T > 18$ GeV, and that the ratio of hadronic to electromagnetic energies (Had/Em) be less than 0.125. This central electron trigger is measured to be (92.8 ± 0.2) % efficient for electrons with $20 < E_T < 150$ GeV. Offline the electromagnetic calorimetry energies are corrected and tighter cuts are imposed to improve the electron identification. A summary of the most important central electron selection criteria are given below.

- TIGHT CENTRAL ELECTRON CUTS

- $|\eta| < 1.0$
- $E_T > 20$ GeV
- $0.5 < E/p < 2.0$
- $\text{Had/Em} < 0.055 + .00045E(\text{GeV})$
- Isolation < 0.1 for $\Delta R = 0.4$

The last criterion imposes a limit on the transverse energy E_{Tcal} (excluding the electron transverse energy E_T) within a cone of $\Delta R = \sqrt{\Delta\phi^2 + \Delta\eta^2} = 0.4$. The isolation variable is defined to be E_{Tcal}/E_T . After these cuts the data sample consists of 32,193 events with at least one good central electron.

A second electron is selected using looser identification criteria. Cuts on the minimum transverse energy E_T depend on the η range defined by the three electromagnetic calorimeters: for $|\eta| < 1.1$, $E_T > 20$ GeV; for $1.1 < |\eta| < 2.4$, $E_T > 15$ GeV; and for $2.2 < |\eta| < 4.2$, $E_T > 10$ GeV.

The $Z \rightarrow e^+e^-$ decay candidates are selected from electron pairs formed from the tightly selected central electron and any of the loosely selected electrons. Electron pairs with the same sign are rejected. Figure 1a shows the resulting electron pair mass spectrum. Finally 1531 events are accepted as $Z \rightarrow e^+e^-$ decay candidates by applying the electron pair mass cut $75.0 < M_{ee} < 105.0$ GeV/c².

2.2 The $Z \rightarrow \mu^+\mu^-$ Data Set

The $Z \rightarrow \mu^+\mu^-$ decays are selected from a data set which includes events with one high energy muon in the region $|\eta| < 0.6$. Level 3 of the on-line trigger requires that a reconstructed track with $p_T > 18$ GeV/c, when extrapolated to the radius of the muon chambers, be matched to a track segment in those chambers to within 10 cm in $r \cdot \Delta\phi$ space. In addition, the energy deposited in the associated hadron calorimeter tower must be less than 6 GeV. The central muon detector (CMU)

covers a pseudorapidity range $|\eta| < 0.6$ and has a trigger efficiency of $(86.8 \pm 1.9) \%$ for muons with $p_T > 20$ GeV/c. Offline a beam constraint is applied to the muon momentum calculation and tighter cuts are imposed to improve muon identification. A summary of the most important tight muon cuts is given below.

- TIGHT CENTRAL MUON CUTS

- $|\eta| < 0.6$
- $p_T(\text{beam constrained}) > 20$ GeV/c
- $|z_{event} - z_\mu| < 5.0$ cm
- electromagnetic energy < 2.0 GeV
- hadronic energy < 6.0 GeV
- $|r \cdot \Delta\phi(CMU)| < 3.0$ cm
- passes a cosmic ray filter

Events with a muon satisfying the tight cuts described above are examined for a second muon. The second muon is selected using looser identification criteria. It must have $p_T > 20$ GeV and must lie within the kinematic region $|\eta| < 1.1$.

The $Z \rightarrow \mu^+\mu^-$ decay candidates are selected from muon pairs formed from the tightly selected muon and any of the loosely selected muons. Muon pairs with the same sign are rejected. Figure 1b shows the resulting muon pair mass spectrum. Finally 580 events are accepted as $Z \rightarrow \mu^+\mu^-$ decay candidates by applying the muon pair mass cut $75.0 < M_{ee} < 105.0$ GeV/c².

2.3 Selection of Jets in the Z Event Sample

The Z boson selection procedure described above provides 2111 candidates for the reaction $\bar{p}p \rightarrow Z + \text{jets}$. These events are examined for jets using a CDF jet reconstruction algorithm [4] which clusters hadronic and electromagnetic calorimeter energies in a cone of fixed radius in $\eta - \phi$ space. A cone size of $R = 0.4$ was chosen for this analysis.

The measured jet energies must be corrected for a variety of instrumental effects such as calorimeter non-linearities and reduced calorimeter response at boundaries between modules and calorimeter subsystems. Additional corrections to the jet energies depend on the cone size used to collect the jet energy and other effects which may depend on the physics process under study. These include out-of-cone losses, undetected energy carried by muons and neutrinos and contributions from the underlying event. The correction factors applied depend on the jet E_T and η , and are meant to reproduce the average jet E_T correctly. Typically the jet energy correction increases a jet's energy by about 30 %. For a detailed discussion of these corrections see references [4] and [5]. We estimate that the combined uncertainty of these corrections introduces an effective 10 % uncertainty on the energy scale of jets.

For this analysis we require that the jets produced with the Z boson have corrected $E_T > 15$ GeV and $|\eta_d| < 2.4$. η_d refers to pseudorapidity measured from the center of the collision region ($z = 0$). Using these requirements we find 248(100) Z + 1 jet events, 60(30) Z + 2 jet events, 9(6) Z + 3 jet events, 4(1) Z + 4 jet events, 1(0) Z + 5 jet events, and 1(0) Z + 6 jet events in the electron(muon) channels.

The jet multiplicity data from the Z + jets events are summarized in Table 1. Figure 2 shows the fraction of events versus jet multiplicity for the electron and muon Z decays. These distributions have not been corrected for efficiency or backgrounds and are meant only to show the general character of the jet multiplicity spectrum.

Table 1: Jet Multiplicities associated with Z production

Jet Mult	Z evts	Fraction
0	1651	0.7821
1	348	0.1649
2	90	0.0426
3	15	0.0071
4	5	0.0024
5	1	0.0005
6	1	0.0005

The E_T spectra of the jets associated with Z production are presented in Section 4, where they are compared to leading order QCD predictions. The features of the QCD calculation, parton fragmentation and detector simulation are discussed below.

3 Monte Carlo Generation of Z + jet Events

3.1 Generation of Z + n parton events

We use the leading-order QCD program VECBOS [2] to generate Z + n parton events with $n = 1, 2$ and 3. The events generated produce the four momenta of the Z boson and n partons, and are an inclusive sum over additional partons. Equal numbers of $Z \rightarrow e^+e^-$ and $Z \rightarrow \mu^+\mu^-$ are simulated in order to properly include the effects of lepton selection cuts.

The Monte Carlo event sample was produced using MRS D0 structure functions and a Q^2 scale equal to $\langle p_T \rangle^2$ where the average is over the p_T of the n partons in the event. The kinematic range used to generate the leptons and partons is given below.

- leptons:
 - $P_T > 12 \text{ GeV}/c$
 - $|\eta| < 4.0$
- jets:
 - $E_T > 8 \text{ GeV}$
 - $|\eta| < 3.0$
 - $\Delta R_{jj} > 0.4$

Each generated event has a weight calculated from the matrix element for that particular $Z + n$ parton event. Based upon the maximum weight in each generated event sample, subsets of events with unit weight are selected for subsequent processing.

3.2 Fragmentation of the partons

The $Z + n$ parton events are converted to $Z + \text{jet}$ events by transforming the partons into jets of particles. For the results presented here we use a scheme based upon color string fragmentation as described by the HERWIG [6] shower program. This has been interfaced to the VECBOS program by a procedure which takes the parton configuration supplied by VECBOS and assigns definite flavors and colors to the partons. Once this is done the colored partons are passed to the HERWIG shower program which evolves the partons, with both initial and final state gluon radiation, and hadronizes the gluons and quarks to produce a complete particle simulation of $Z + \text{jet}$ events. This fragmentation procedure, called HERPRT, is described in detail in reference [7].

3.3 Generation of detected $Z + \text{jet}$ events

The $Z + \text{jet}$ events, with the particle structure described above, are introduced into a model of the CDF detector. This simulation produces the response of the electromagnetic and hadronic calorimeters and muon detectors, and creates output banks with the same format as the data. Jets are reconstructed in these Monte Carlo events using the algorithm described in Section 2.3. Finally the reconstructed jets and leptons are subjected to the selection cuts applied to the data, using the same analysis program.

In the process of parton fragmentation, jet reconstruction and final jet selection, an event generated with $Z + n$ partons may be detected as an event with $Z + m$ jets where m can be either less than n (for events in which jets are removed by cuts) or greater than n (for events in which additional gluon radiation is generated by HERWIG). When comparing to a data sample with $Z + \geq n$ jets we use the VECBOS

prediction for $Z + n$ partons but keep only those events which pass all our selection cuts with $m \geq n$.

4 Jet Production Properties in $Z + \text{jet}$ Events

4.1 Inclusive jet E_T spectra

The $Z + \text{jets}$ data sample consists of 460 $Z + \geq 1$ jet events, 112 $Z + \geq 2$ jet events, and 22 $Z + \geq 3$ jet events. As described in Section 2.3, the jets are restricted to the kinematic region $|\eta_d| < 2.4$ with $E_T > 15$ GeV. For events with multiple jets we order the jets from highest transverse energy to lowest: E_{T1} , E_{T2} , etc.

The E_{T1} spectrum for the $Z + \geq 1$ jet events is shown in Figure 3a). The data, indicated by the points with errors, extend out to a jet E_T of 198 GeV (the last bin from 150 to 200 GeV contains 2 events). The histogram is the leading order QCD prediction starting from the VECBOS $Z + 1$ parton generation, with the fragmentation effects and detector simulation described in Section 3. The E_{T1} spectra for the $Z + \geq 2$ jet and $Z + \geq 3$ jet events are shown in Figures 3b) and 3c). These are compared respectively to the VECBOS $Z + 2$ parton and $Z + 3$ parton simulations. In these comparisons the VECBOS predictions have been normalized to the number of events in each data sample. The QCD predictions agree well with the data except for a possible underestimate at the highest E_T rate in the $Z + \geq 1$ jet events. Studies are in progress to measure the sensitivity of the VECBOS predictions to the choice of Q^2 and structure functions.

The E_T spectra of the second (E_{T2}) and third (E_{T3}) most energetic jets produced in $Z + \geq 2$ jet and $Z + \geq 3$ jet events are shown in Figure 4. Within the limited statistics, the VECBOS predictions agree with the measured E_T spectra.

4.2 Correlations between jet E_T

The correlation between E_{T2} and E_{T3} of the jets in the 22 $Z + \geq 3$ jet events is shown in Figure 5. Figure 5a) shows a scatter plot of the VECBOS prediction for E_{T2} vs E_{T3} and Figure 5b) the scatter plot for the data. The dashed line in these figures is at $E_{T2} + E_{T3} = 48$ GeV. This divides the number of VECBOS events into two equal parts. Nine out of the 22 data points fall above the dashed line, consistent with the prediction of 50%. The sum of E_{T2} and E_{T3} is shown in Figure 5c), where the data agree with the VECBOS prediction.

4.3 B-tags in $Z + \text{jet}$ events

The CDF collaboration has developed two tagging methods to search for B hadron decays in jets. The first, referred to as SVX tagging, makes use of CDF's silicon tracker to search for secondary decay vertices which could signal the presence

of a b or c quark decay. The second method searches for the soft electrons or muons arising from the leptonic decays of b quarks (or the sequential c quarks). This is referred to as soft lepton tagging (SLT). These tagging algorithms, described in detail in references [8] and [9], have been shown to be effective in identifying B hadrons and measuring their average lifetime [8].

We have applied these B-tag algorithms to a subsample of Z events with multiple jets and high jet transverse energy. The events selected are nine $Z + \geq 3$ jet events with $E_{T2} + E_{T3}$ above a cut at 48 GeV which, according to VECBOS, divides the data set into two equal parts. This cut is indicated as the dashed line in the E_{T2} vs E_{T3} scatter plot shown in Figure 5b). In this data sample, two events are found to have SVX tags and none SLT tags. The tagged events are shown as the open squares in Figure 5b).

The tags observed in these nine $Z + \geq 3$ jet events can be compared to predictions made from the tagging rates measured for similar jets from generic QCD events. The generic QCD tagging rates include mistags and the small contributions from residual K_s and Λ decays, in addition to the contributions from the actual heavy flavor content in the jets. Applying these jet tagging estimates to the jets in the nine $Z + \geq 3$ jet events, 0.44 events are predicted to have SVX tags and 0.48 SLT tags. The uncertainties in these predictions is about 15%. The probability that the 0.44 predicted SVX tags fluctuate up to the two observed is 7%. Adding the SVX and SLT tags, 0.92 tags are predicted with 2 observed (a probability of 23%). Therefore we observe no statistically significant excess heavy flavor content in the jets from these $Z +$ jet events over that observed in generic QCD jets. A quantitative comparison of the B hadron content expected in jets associated with Z bosons awaits a detailed study of backgrounds to our event sample. This is in progress, along with a more global search for B hadrons in all $Z +$ jet events.

5 Summary

The properties of QCD jets produced in association with Z bosons in 1.8 TeV $\bar{p}p$ collisions have been measured using the CDF detector. The E_T spectra in the region $|\eta_d| < 2.4$ with $E_T > 15$ GeV are compared to leading order QCD predictions as calculated with the Monte Carlo program VECBOS. In general, the inclusive E_T spectra and E_T correlations are in good agreement with the QCD predictions. The jets in a sample of events with ≥ 3 jets and high sum E_T have been examined for B hadrons. The tag rate observed is consistent with that predicted from generic QCD jets. More detailed studies of the jet structure in these $Z +$ jet events are in progress.

6 Acknowledgments

We thank the Fermilab staff and the technical staffs of the CDF institutions for their vital contributions to this work. We would also like to thank Walter Giele for very useful discussions of the VECBOS QCD calculations. This work was supported by the U.S. Department of Energy and National Science Foundation; the Italian Istituto Nazionale di Fisica Nucleare; the Ministry of Science, Culture, and Education of Japan; the Natural Sciences and Engineering Research Council of Canada; the A.P. Sloan Foundation; and the Alexander von Humboldt-Stiftung.

References

- [1] Contact person A.T.Goshaw, Duke University: email address 47312::GOSHAW.
- [2] F. A. Berends, W. T. Giele, H. Kuijf, and B. Tausk, Nucl. Phys. B357, 32(1991).
- [3] F. Abe et al., Nucl. Instrum. Methods, Sect. A 271,387 (1988).
- [4] F. Abe et al., Phys. Rev. D 45, 1448 (1992).
- [5] F. Abe et al., Phys. Rev. D 47, 4857 (1993).
- [6] G. Marchesini and B. R. Weber, Nucl. Phys. B310, 461 (1988).
- [7] J. M. Benlloch et al., CDF note CDF/DOC/MONTECARLO/1823 (1992).
- [8] F. Abe et al., Phys. Rev. Lett. 71, 3421 (1993).
- [9] F. Abe et al., FERMILAB-PUB-94/097-E (submitted to Phys. Rev. D).

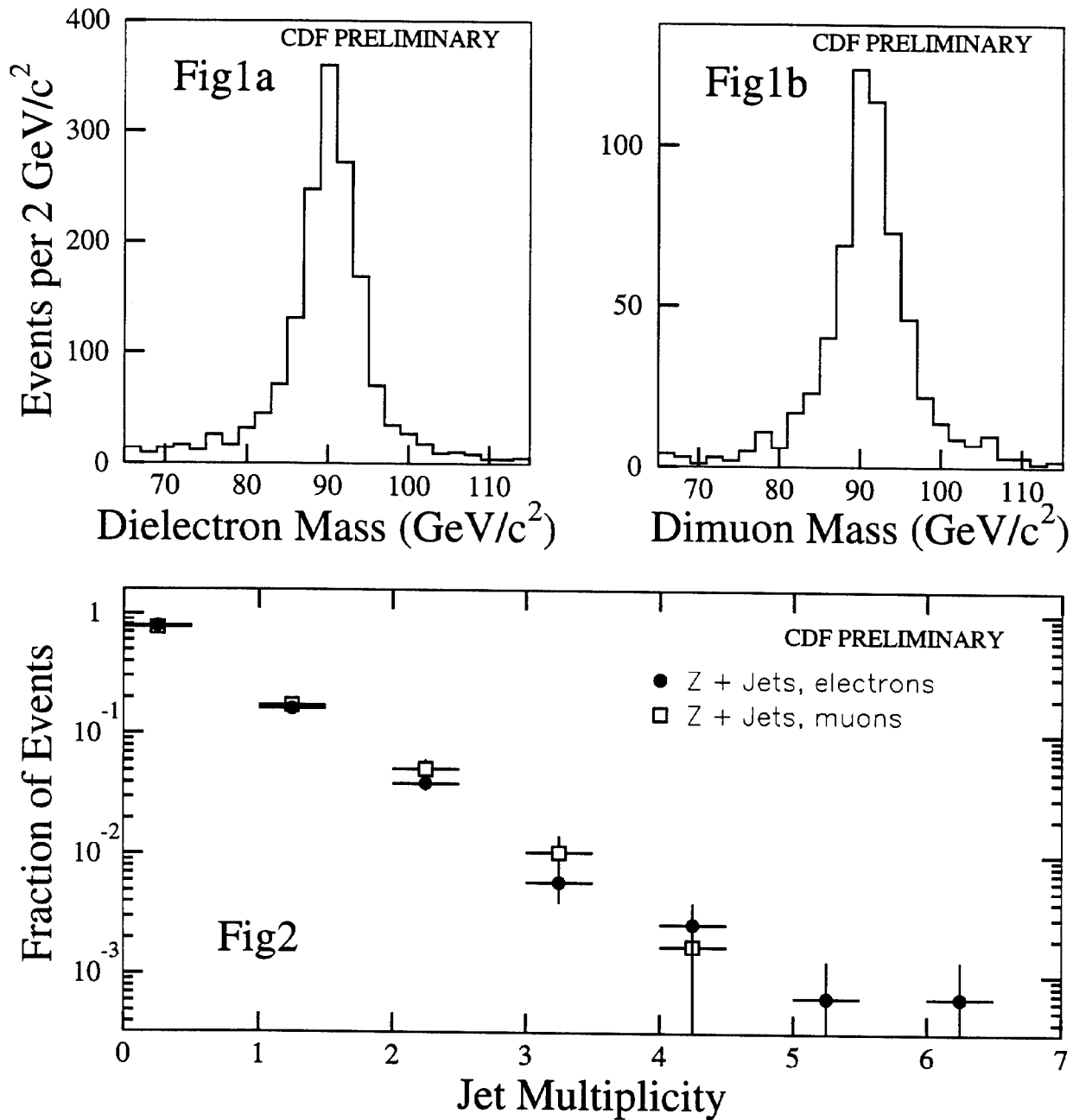


FIG. 1. Dilepton invariant mass distributions separated into a) electrons, b) muons.
 FIG. 2. Fraction of Z + jet events versus jet multiplicities.

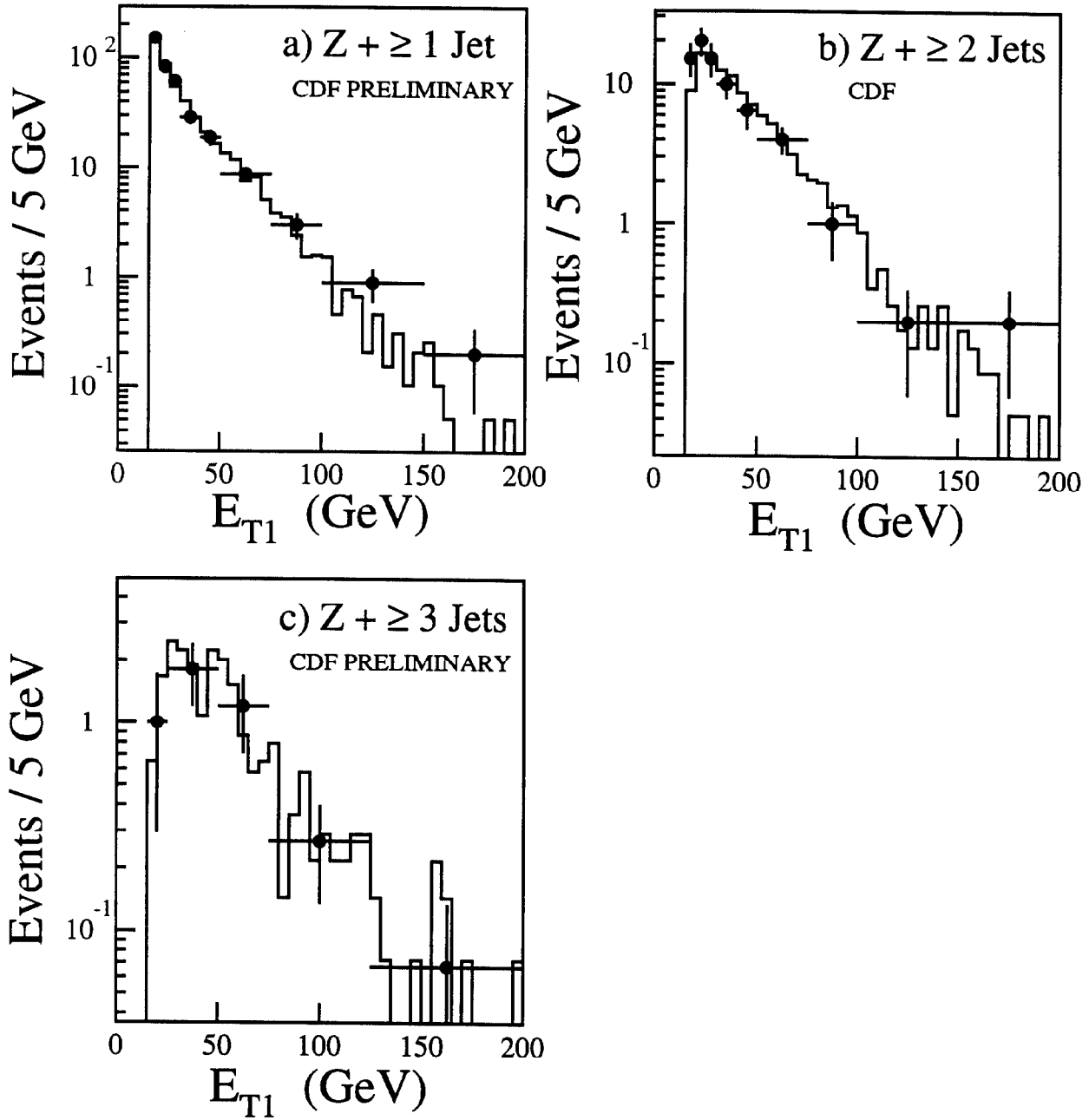


FIG. 3. The jet E_{T1} spectra for a) $Z + \geq 1$ jet events; b) $Z + \geq 2$ jet events; and c) $Z + \geq 3$ jet events.

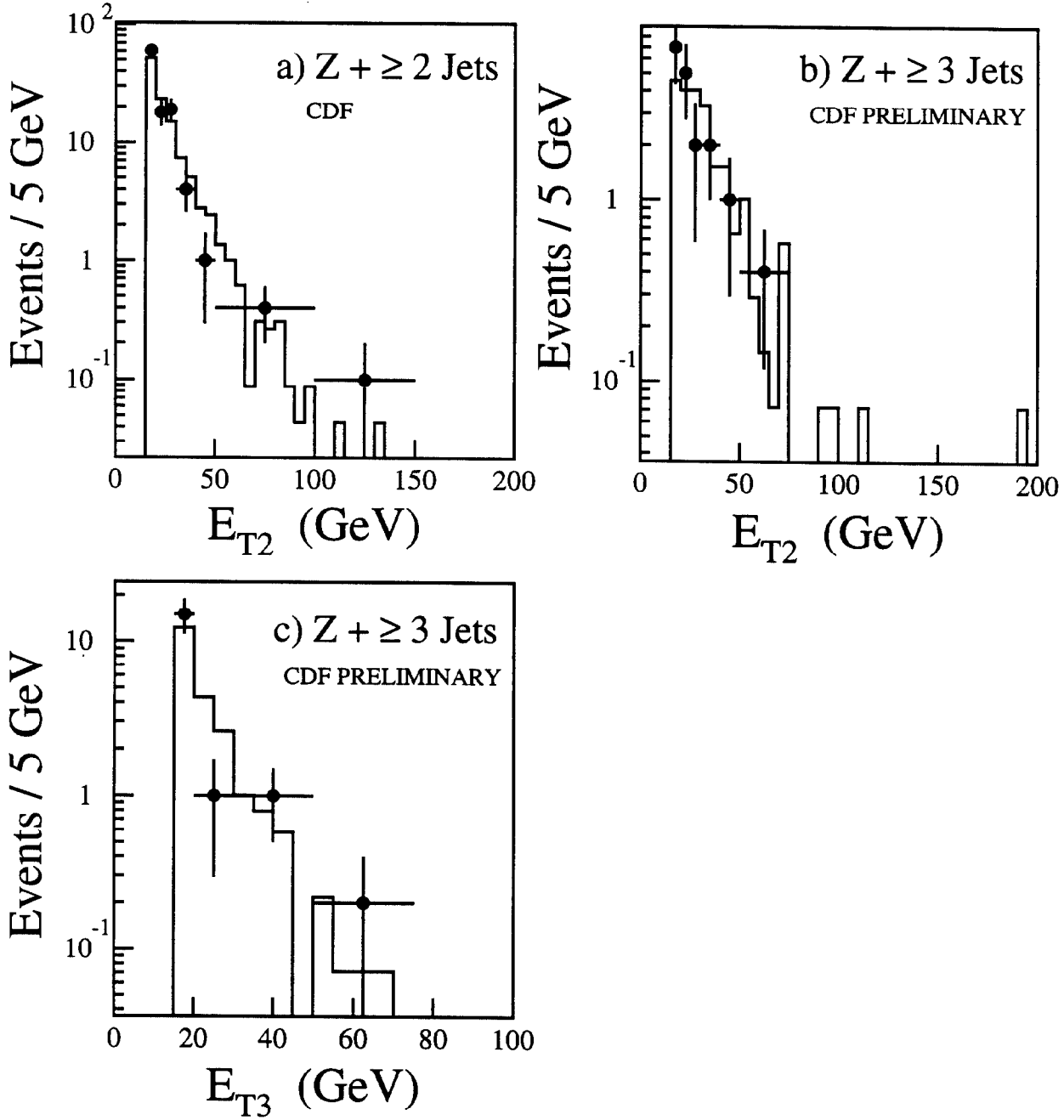


FIG. 4. The E_{T2} spectra for a) $Z + \geq 2$ jet and b) $Z + \geq 3$ jet events; c) shows the E_{T3} spectrum for $Z + \geq 3$ jet events.

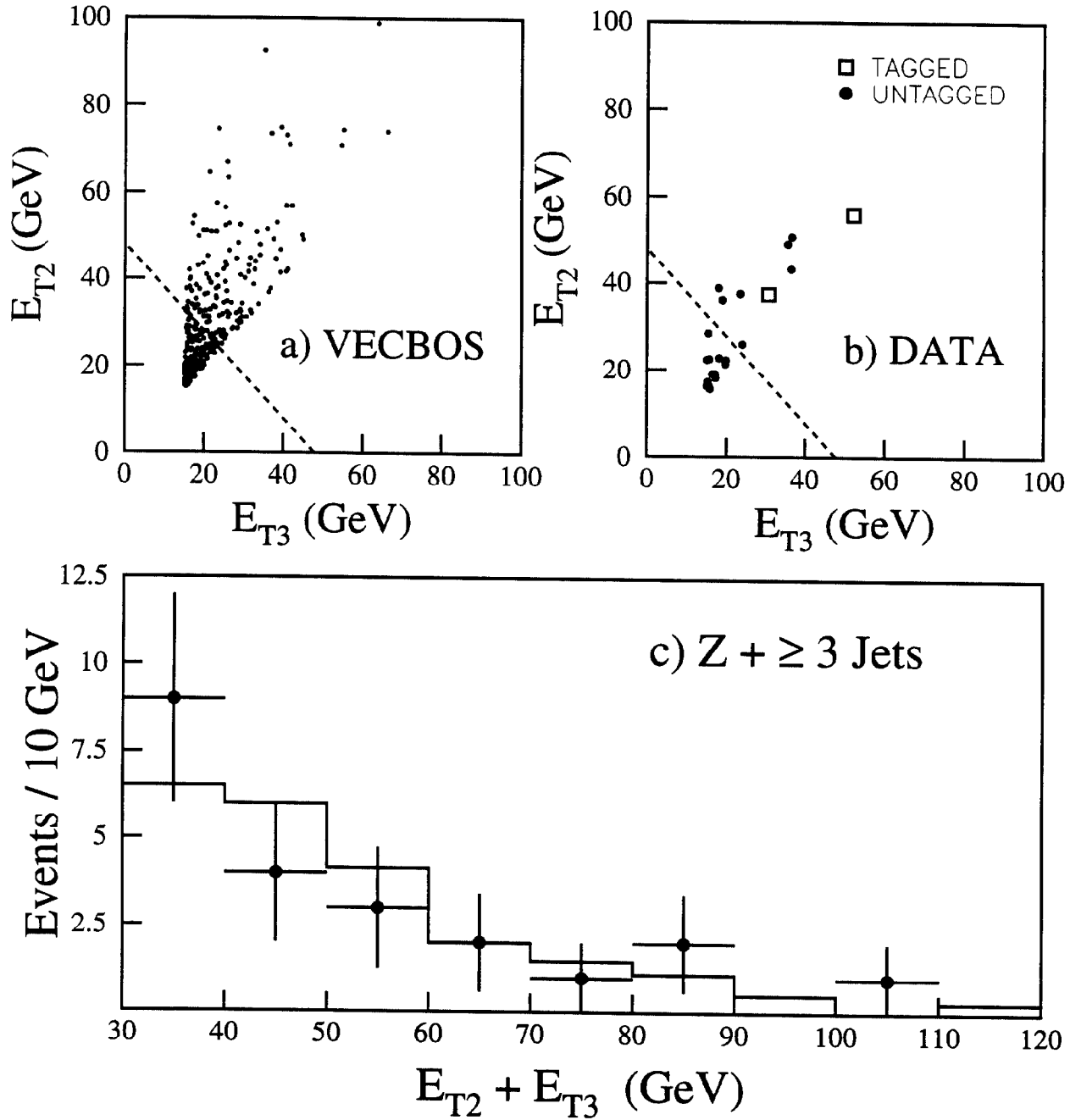


FIG. 5. Scatterplots of E_{T2} vs. E_{T3} a) as predicted by VECBOS and b) as found in the data. The SVX tagged events are shown as open squares. The dashed line in a) and b) is given by the function $E_{T2} + E_{T3} = 48$ GeV and defines the sum above which 50% of the VECBOS events fall. c) $E_{T2} + E_{T3}$ for the data (points) and VECBOS (histogram).